Temperature and Guanidine Hydrochloride Dependence of the Structural Stability of Ribonuclease T_1†

Isabel M. Plaza del Pino,‡,§ C. Nick Pace,‖ and Ernesto Freire*,‡

Department of Biology and Biocalorimetry Center, The Johns Hopkins University, Baltimore, Maryland 21218, and Department of Medical Biochemistry and Genetics and Department of Biochemistry, Texas A&M University, College Station, Texas 77843

Received June 23, 1992; Revised Manuscript Received September 4, 1992

ABSTRACT: The thermal unfolding of ribonuclease T_1 has been studied by high-sensitivity differential scanning calorimetry as a function of temperature, [GuHCl], and scanning rate. The destabilizing effect of GuHCl has revealed that the kinetics of the unfolding transition become extremely slow as the transition temperature decreases. At pH 5.3 and zero GuHCl, the unfolding transition is centered at 59.1 °C; upon increasing the GuHCl concentration, the transition occurs at lower temperatures and exhibits progressively slower kinetics; so, for example, at 3 M GuHCl, the transition temperature is 40.6 °C and is characterized by a time constant close to 10 min. Under all conditions studied (pH 5.3, pH 7.0, [GuHCl] < 3 M), the transition is thermodynamically reversible. The slow kinetics of the transition induce significant distortions in the shape of the transition profiles that can be mistakenly interpreted as deviations from a two-state mechanism. Determination of the thermodynamic parameters from the calorimetric data has required the development of an analytical formalism that explicitly includes the thermodynamics as well as the kinetics of the transition. Using this formalism, it is shown that a two-state slow-kinetics model is capable of accurately describing the structural stability of ribonuclease T_1 as a function of temperature, GuHCl concentration, and scanning rate. Multidimensional analysis of the calorimetric data has been used to estimate the intrinsic thermodynamic parameters for protein stability, the interaction parameters with GuHCl, and the time constant for the unfolding transition and its temperature dependence.

Ribonuclease T_1 (RNase T_1) from *Aspergillus orizae* is one of the best-studied microbial enzymes. It is a small globular protein (104 amino acids residues) and occurs as a mixture of 2 isoforms with either Gln or Lys at position 25 (Gln25-RNase T_1 or Lys25-RNase T_1). Most solution studies have used the Gln25 isoenzyme. However, the first (Heinemann & Saenger, 1982) and some of the more recent crystal structures (Arni et a., 1987, 1988; Koepke et al., 1989; Kostrewa et al., 1989; Martinez-Oyanedel et al., 1991) of RNase T_1 have been obtained for Lys25-RNase T_1. The secondary structure of this protein consists of a short 2-stranded antiparallel β-sheet followed by 1 extended α-helix of 4.5 turns and a second antiparallel β-sheet composed of 5 strands. These elements are connected by extended "loop" regions. The polypeptide chain is cross-linked by 2 disulfide bonds which form a small (2–10) and a large (6–103) loop.

RNase T_1 has proven to be an excellent model for investigating several aspects of protein folding. It folds and is enzymatically active with one or both disulfide bonds broken and the cysteines carboxymethylated (Pace et al., 1988). An increase in ionic strength leads to a surprisingly strong increase in stability (Oobatake et al., 1979; Pace & Grimsley, 1988). The kinetic mechanism of folding of Lys25-RNase T_1 is characterized by three major phases: a rapid phase that is completed within seconds and two slow phases in the range of minutes to hours (Kiefhaber et al., 1990a,b). The slow phases have been attributed to proline isomerization (Kiefhaber et al., 1990c). It has also been observed that the guanidine hydrochloride (GuHCl)-induced unfolding reaction is extremely slow at 10 °C (Kiefhaber et al., 1990a) and that this behavior appears to be related to prolyl isomerization (Kiefhaber & Schmid, 1992). The replacement of Gln25 with Lys has no effect on the activity of RNase T_1, and the two forms of the enzyme have identical substrate specificities (Heinemann et al., 1980; Shirley et al., 1989). This is not surprising because this residue is on the opposite side of the molecule from the active site, and the substitution has very little effect on the overall shape of the molecule (Sugio et al., 1988). Despite this fact, Shirley et al. (1989) have shown that Lys25-RNase T_1 is more stable than Gln25-RNase T_1. This is also evident from the DSC studies on Lys25-RNase T_1 by Kiefhaber et al. (1990), and on Gln25-RNase T_1 by Hu et al. (1992).

In this paper, we present the results of a systematic characterization of the structural stability of Lys25-RNase T_1 using multidimensional differential scanning calorimetry as a function of temperature, scanning rate, and the concentration of GuHCl. These studies demonstrate the existence of GuHCl-mediated kinetic effects on the folding/unfolding transition. Contrary to the situation existing with other proteins, GuHCl not only has a destabilizing effect on Lys25-RNase T_1 but it also reveals a significant effect on the rate of the unfolding transition as the transition is shifted to lower temperatures. At moderate concentrations of GuHCl (<3 M), the thermal transition becomes increasingly slow and characterized by relaxation times on the order of several minutes. Multidimensional analysis of the heat capacity data has allowed resolution of the thermodynamic and kinetic parameters that characterize the thermal unfolding transition. In the past, different procedures have been developed for the deconvolution analysis of protein transitions that do not exhibit

† Supported by National Institutes of Health Grants RR04328, GM37911, and NS24520 (E.F.) and Grant GM37039 (C.N.P.), by Robert A. Welch Foundation Grant A-1060 and the Tom and Jean McMullin Professorship (C.N.P.), and by a postdoctoral fellowship from the Spanish Ministry of Education and Science (I.M.P.d.P.).

* To whom correspondence should be addressed.

‡ The Johns Hopkins University.

§ Present address: Departamento de Quimica Fisica, Universidad de Granada, Granada, Spain.

‖ Texas A&M University.

0006-2960/92/0431-11196$03.00/0

classical two-state behavior and exhibit partially folded states (Freire & Biltonen, 1978; Freire, 1989; Xie et al., 1991) or exhibit irreversible denaturation (Sanchez-Ruiz et al., 1988). To the best of our knowledge, this is the first time that the calorimetric data associated with a reversible protein unfolding transition that exhibits extremely slow kinetics have been observed and analyzed.

MATERIALS AND METHODS

Protein. Lys25-RNase T_1 was purified as described previously (Shirley et al., 1989; Shirley & Laurents, 1990). MES and MOPS buffers at a concentration of 30 mM were used for thermal unfolding experiments at pH 5.3 and 7.0, respectively. The enzyme was dissolved in the appropriate buffer and dialyzed overnight against 4000 volumes of the same buffer at 4 °C. Protein concentrations were determined spectrophotometrically by using an absorbance of 1.67 at 278 nm for a 1 mg/mL solution in 30 mM MOPS buffer, pH 7.0 (1-cm path length) (Hu et al., 1992). GuHCl stock solutions were prepared in the appropriate protein buffers, the pH was checked and adjusted, and the concentration was determined by refractive index measurements (Pace, 1986; Ramsay & Freire, 1990). Samples to be scanned in the calorimeter or in the spectropolarimeter were prepared by mixing stock RNase T_1 after dialysis with stock GuHCl solution to make a solution containing the desired GuHCl and protein concentrations. The solutions were incubated for a minimum of 20–36 h at 4 °C (DSC) or 25 °C (CD) prior to the performance of the experiments.

Differential Scanning Calorimetry. All calorimetric experiments were performed with a Microcal MC-2 differential scanning calorimeter. The calorimetric unit was interfaced to an IBM PC microcomputer using an A/D converter board (Data Translation DT-2801) for automatic data collection and analysis. The samples were degassed for 15 min at room temperature prior to being scanned. For each GuHCl concentration, three sets of experiments were performed at scan rates of 90, 60, and 20 °C h^{-1}. The protein concentration for these experiments was 1.5–3 mg mL^{-1}. Excess heat capacity functions were obtained after base-line subtraction, as described earlier (Freire & Biltonen, 1978; Freire, 1989; Ramsay & Freire, 1990). All data analysis was performed with software developed at the Biocalorimetry Center.

Circular Dichroism. The spectra were obtained with a JASCO J-710 spectropolarimeter equipped with a jacketed cell of 0.05-cm path length (peptide CD) or with a cell of 1-cm path length using a thermostated cell holder (aromatic CD). All the spectra were measured at a constant temperature of 25 °C by circulating water with an external bath. The temperature reading was accurate to ±0.1 °C. The protein concentration was 0.5 mg mL^{-1} (peptide CD) and 1 mg mL^{-1} (aromatic CD). The ellipticity is expressed as degrees centimeter squared per decimole normalized to the mean residual molecular weight of ribonuclease T_1 (Sander & Ts'o, 1971). The ellipticities at 222 and 285 nm were measured again several hours after the experiments in order to check that the samples were at equilibrium.

RESULTS AND DISCUSSION

Differential Scanning Calorimetry. The DSC thermograms obtained at a scanning rate of 60 °C h^{-1} for the thermal unfolding of ribonuclease T_1 at pH 7.0 and 5.3 are shown in Figure 1. At pH 7.0, the transition is characterized by a T_m, defined as the peak maximum in the apparent heat capacity function, of 53.3 °C whereas at pH 5.3 the T_m is 60.7 °C.

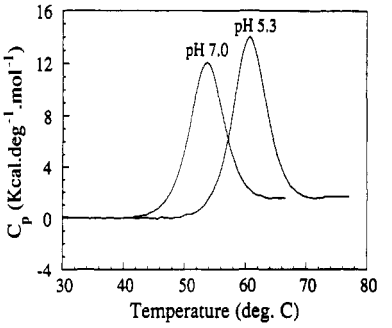

FIGURE 1: Heat capacity function versus temperature for Lys25-RNase T_1 at pH 5.3 (30 mM MES) and at pH 7.0 (30 mM MOPS). The calorimetric scans were performed at a scanning rate of 60 °C h^{-1} at a protein concentration of 2 mg mL^{-1}.

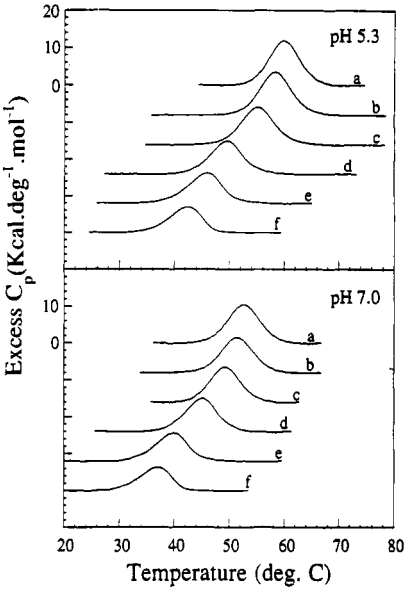

FIGURE 2: Transition excess heat capacity curves versus temperature for Lys25-RNase T_1 at pH 5.3 and 7.0 and at increasing GuHCl concentrations. The calorimetric scans were performed at 20 °C h^{-1} with protein concentrations ranging between 1.5 and 3 mg mL^{-1}. The molar GuHCl concentrations were as follows: for pH 5.3, 0 (a), 0.5 (b), 1.0 (c), 1.8 (d), 2.4 (e), and 3.0 (f); for pH 7.0, 0 (a), 0.7 (b), 1.0 (c), 1.8 (d), 2.3 (e), and 3.0 (f). The curves have been displaced in the y axis for display purposes.

These T_m's are in reasonable agreement with the values obtained previously by optical spectroscopy (Shirley et al., 1989) and calorimetry (Kiefhaber et al., 1990d). The apparent enthalpy changes, uncorrected for the ionization enthalpy of the buffers, are 84.5 and 92.5 kcal mol^{-1} for the experiments at pH 7.0 and 5.3, respectively. At the two pHs studied, the ratios of the van't Hoff to the calorimetric enthalpies are about 1.3. This deviation from the expected value of 1 for a two-state transition has been observed before for ribonuclease T_1 even though no obvious explanation could be found (Hu et al., 1992). Also, the transition is characterized by a ΔC_p of 1.6 ± 0.2 kcal K^{-1} mol^{-1} in agreement with previous estimates obtained under similar conditions (Kiefhaber et al., 1990d; Hu et al., 1992). In both cases, the transition is completely reversible as demonstrated by the reappearance of the entire signal upon repeated scans of the same samples.

Figure 2 shows the entire family of calorimetric scans obtained at a scanning rate of 20 °C h^{-1} and increasing concentrations of GuHCl. The excess heat capacity curves shown in the figure were obtained after base-line subtraction as described before (Ramsay & Freire, 1990; Straume & Freire, 1992). As expected, the transition temperature

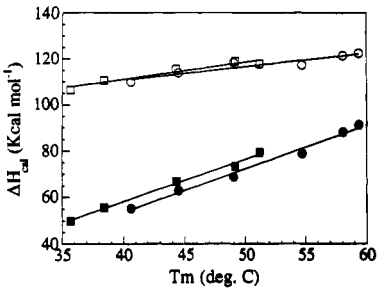

FIGURE 3: Calorimetric (solid symbols) and van't Hoff (open symbols) enthalpies as a function of temperature for the experiments performed at pH 5.3 (circles) and pH 7.0 (squares). The transition temperatures are the equilibrium values obtained by extrapolating the experimental values (Figure 5) to zero scanning rate. The enthalpy values are the mean of three scans performed at 20, 60, and 90 °C h^{-1} for each GuHCl concentration.

decreases at increasing concentrations of the denaturant. At pH 7.0, the T_m decreases 16 °C upon increasing the GuHCl concentration to 3 M; at pH 5.3, the decrease in T_m is on the order of 19 °C. A plot of the calorimetric enthalpy change versus the transition temperature for the experiments obtained at different GuHCl concentrations indicates a linear dependence as shown in Figure 3. For the two pHs studied, the slopes (ΔC_p) are similar and equal to 1.8 ± 0.1 kcal K^{-1} mol^{-1}. This value is slightly higher than the values obtained in the absence of GuHCl. In this respect, Makhatadze and Privalov (1992) have also noticed that the ΔC_p for several proteins is slightly larger in the presence of GuHCl. One possible molecular interpretation is that in the presence of GuHCl there is a reduced exposure of protein polar groups to the solvent upon unfolding due to the binding of GuHCl. Since the contribution of the exposure of polar groups to the overall ΔC_p is negative (Makhatadze & Privalov, 1990; Murphy & Gill, 1991), a reduced exposure of polar groups should result in a larger ΔC_p.

It should be noted that at similar temperatures, the enthalpy values obtained at pH 5.3 are approximately 7 kcal mol^{-1} lower than those obtained at pH 7.0. This can be interpreted in terms of the known protonation behavior of the three histidines and two glutamic acids present in ribonuclease T_1. The three histidines in ribonuclease T_1 have anomalously high pK_a's of 7.8, 7.9, and 7.2 in the native form (Inagaki et al., 1981; McNutt et al., 1990). Therefore, at pH 7.0, the unfolding transition is expected to be associated with the deprotonation of these histidines or at least two of them. Since the enthalpy of ionization of histidine is 7 kcal mol^{-1} and the enthalpy of protonation of the buffer MOPS is −5 kcal mol^{-1}, a difference of 4–6 kcal mol^{-1} is expected from this effect between the experiments at pH 7.0 and 5.3. This calculation assumes that the enthalpies of ionization of the anomalous histidines are similar to those of standard histidines. It should also be noted that ribonuclease T_1 apparently has two glutamic acids with pK_a's of 5.5 and 5.7 (Pace et al., 1990). These groups are expected to be half-protonated in the native state at pH 5.3 and essentially unprotonated in the unfolded state. The enthalpy of ionization of glutamic acid is negligible; however, the enthalpy of protonation of the buffer MES is −3.71 kcal mol^{-1}. Therefore, an overall difference of 7–9 kcal mol^{-1} in ΔH is expected between the experiments at pH 7.0 and 5.3, in close agreement with the observed results.

The most notable feature of the data in Figure 2 is that the calorimetric curves become progressively asymmetric toward the low-temperature end of the transition at increasing GuHCl concentrations. This effect of GuHCl results in an increasingly higher $\Delta H_{vh}/\Delta H$ ratio at higher GuHCl concentrations as also indicated in Figure 3. Numerically, the cause of the increased $\Delta H_{vh}/\Delta H$ ratio is a smaller than expected decrease in the van't Hoff enthalpy at higher GuHCl concentrations; i.e., the van't Hoff heat capacity change is less than the calorimetric heat capacity change. It should be noted that the ΔC_p value obtained from the temperature dependence of the calorimetric enthalpy coincides within error with the one obtained directly from the calorimetric traces. This effect should be contrasted with the one observed previously for apo-α-lactalbumin (Xie et al., 1991). In that case, the $\Delta H_{vh}/\Delta H$ also increases at high GuHCl concentrations; however, the effect is due to a larger than expected decrease in the calorimetric enthalpy and not to a smaller than expected decrease in the van't Hoff enthalpy. For apo-α-lactalbumin, the ΔC_p calculated from the temperature dependence of the van't Hoff enthalpy is close to the values obtained directly from the calorimetric traces.

There are several potential molecular causes for the observed effect of GuHCl on the shape of the transition curves for ribonuclease T_1. First is the possibility of transition irreversibility at high GuHCl concentrations, second is the possibility that higher order cooperative aggregates are formed at high GuHCl concentrations, third is the possibility of some GuHCl-induced changes in the transition mechanism, and fourth is the possibility of kinetic effects evident at high GuHCl concentrations. Each of these possibilities was checked experimentally in order to evaluate the origin of the observed effect.

Origin of the Apparent Deviation from the Two-State Mechanism. The condition of thermodynamic equilibrium was checked for all experimental conditions studied in this paper by scanning each sample twice. At pH 5.3, the calorimetric scans were more than 90% reversible up to 2.5 M GuHCl. At pH 7.0, the scans were better than 70% reversible up to 2.5 M GuHCl. The reversibility of the transition decreased to less than 40% only at GuHCl concentrations higher than 3 M. Therefore, the observed asymmetry in the transition and the resulting high $\Delta H_{vh}/\Delta H$ ratios cannot be attributed to transition irreversibility within the GuHCl concentration range studied. This is especially true for the data at pH 5.3 in which the transition is better than 90% reversible even though the $\Delta H_{vh}/\Delta H$ ratio is approximately 2 at 2.5 M GuHCl.

The possibility of higher order cooperative aggregates was discarded by performing experiments at different protein concentrations. Protein concentration did not have an effect on the shape of the calorimetric profiles. Also, the transition temperatures obtained calorimetrically are similar to the transition temperatures obtained spectroscopically at concentrations about 10 times lower (Kiefhaber et al., 1990).

The possibility of an altered transition mechanism was examined by circular dichroism. CD spectra in the 195–250-nm region and the 235–315-nm region were obtained at different GuHCl concentrations in order to investigate whether changes in tertiary structure occur prior to changes in secondary structure, as expected for the formation of partially folded molten globule intermediates (Kuwajima, 1989). The results of such experiments are shown in Figure 4 in which the ellipticities at 222 and 285 nm have been plotted as a function of GuHCl concentration. As shown in the figure, the midpoint of the transition is the same, regardless of the wavelength used to monitor the unfolding process. At pH 7.0 and 25 °C, the midpoint of the GuHCl-induced transition occurs at 3 M; at pH 5.3, the midpoint occurs at 3.7 M, in excellent agreement with previously reported values (Kiefhaber

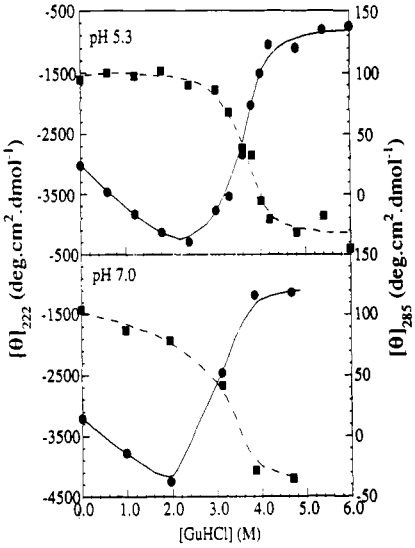

FIGURE 4: Ellipticity at 222 (solid circles) and 285 nm (solid squares) versus GuHCl concentration at pH 5.3 and 7.0. All the spectra were measured at 25 °C using identical buffer conditions as in the calorimetric scans.

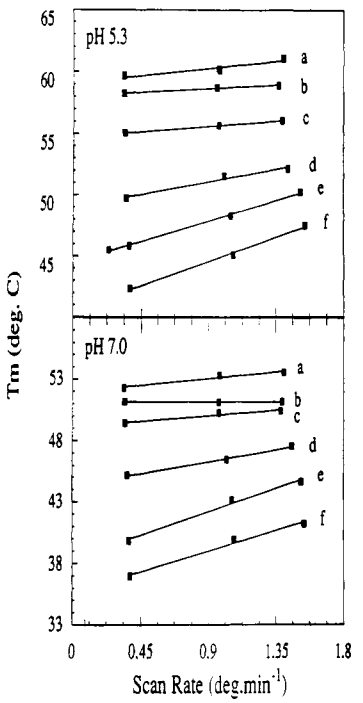

FIGURE 5: Experimental transition temperatures versus scanning rate at pH 5.3 and 7.0 and different GuHCl concentrations. The molar GuHCl concentrations are the same as in Figure 2. For pH 5.3, 0 (a), 0.5 (b), 1.0 (c), 1.8 (d), 2.4 (e), and 3.0 (f); for pH 7.0, 0 (a), 0.7 (b), 1.0 (c), 1.8 (d), 2.3 (e), and 3.0 (f).

et al., 1990a). These results indicate that the secondary structure (195–250 nm) and the tertiary structure (235–315 nm) are disrupted simultaneously, contrary to the case in which molten globules are formed (Kuwajima, 1989). In those cases, the tertiary structure of the protein is disrupted prior to the secondary structure.

The possibility of kinetic effects was checked by repeating the calorimetric experiments at different scanning rates. It was immediately apparent that the transition temperatures were strongly dependent on the scanning rate, as expected for a transition exhibiting slow kinetics (Lentz et al., 1978). Figure 5 shows the scanning rate dependence of the transition temperature (defined as the temperature of the heat capacity maximum) for each of the experimental conditions considered in this study. At zero GuHCl, the transition temperature is only slightly dependent on the scanning rate; it varies about 1 °C upon varying the scanning rate from 20 to 90 °C/h. At low GuHCl concentrations (0.5 M), the transition temperature becomes almost independent of the scanning rate, and finally at higher GuHCl concentrations, the transition temperature becomes strongly dependent on the scanning rate at both pH 5.3 and pH 7.0. These experiments demonstrate that the transition is kinetically slow since variations in the scanning rate affect the temperature location of the peaks. A phenomenological analysis of the T_m dependence on the scanning rate as described by Lentz et al. (1978) indicates that the time constant for the thermal unfolding transition is longer than 6 min at the higher GuHCl concentrations. It was therefore decided to investigate whether the slow kinetics of the transition were responsible for the observed distortion in the shape of the heat capacity curves.

Multidimensional Modeling of Transition Curves Including Kinetic Effects. As discussed before, the basic quantity required to interpret calorimetric data is the excess enthalpy function ($\langle \Delta H \rangle$) which is directly proportional to the population of molecules that have undergone unfolding or partial unfolding (Freire & Biltonen, 1978; Freire & Murphy, 1991). The excess heat capacity function measured by differential scanning calorimetry is simply the temperature derivative of $\langle \Delta H \rangle$. In general, $\langle \Delta H \rangle$ is given by the equation:

$$\langle \Delta H \rangle = \sum P_i \Delta H_i \qquad (1)$$

where P_i is the population of protein molecules in the ith state and ΔH_i the enthalpy difference between that state and the reference state, taken as the native state, and the summation is over all the states that become populated in the transition. For a two-state transition, the above equation reduces to $\langle \Delta H \rangle = P_u \Delta H$, where P_u is the population of molecules in the unfolded state.

A calorimetric scan performed at a constant scanning rate can be considered as a long succession of equally spaced very small temperature jumps. At each temperature, the population of molecules in the unfolded state can be written in terms of its equilibrium value and a set of relaxation equations. Since a calorimetric scan begins after a long equilibration period (1 h or more) at a specific temperature (T), the initial population distribution at the beginning of the scan can be assumed to correspond to the equilibrium situation. At the next instant in time ($t + \Delta t$), the temperature would have changed to $T + \alpha \Delta t$, where α is the scanning rate. At this new temperature, the actual population of molecules $[P'_u(T + \alpha \Delta t)]$ will be a function of the expected equilibrium value at the new temperature $[P_u(T + \alpha \Delta t)]$ and the relaxation kinetics of the system:

$$P'_u(T + \alpha \Delta t) = P_u(T + \alpha \Delta t) + [P'_u(T) - P_u(T + \alpha \Delta t)] \exp(-k \Delta t) \qquad (2)$$

where the rate constant k is also expected to be a function of temperature and the denaturant concentration. The use of a linearized rate equation is justified because each temperature perturbation is arbitrarily small (Eigen, 1963). The above equation can be written in a recursive form as

$$P'_u(T_{i+1}) = P_u(T_{i+1}) + [P'_u(T_i) - P_u(T_{i+1})] \exp(-k \Delta T/\alpha) \qquad (3)$$

At the initial temperature in the scan, T_0, the observed population of molecules in the unfolded state is equal to the

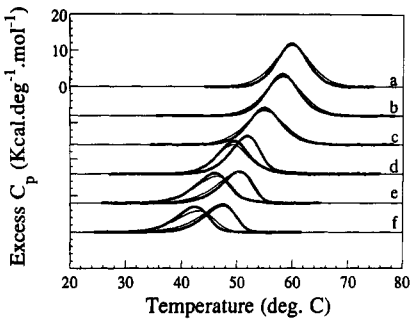

FIGURE 6: Transition excess heat capacity curves versus temperature obtained at increasing GuHCl concentrations, different scanning rates, and constant pH 5.3. The molar concentrations of GuHCl are the same as in Figure 2. The scanning rates are 20 °C h^{-1} (a–c) and 20 and 90 °C h^{-1} (d–f). The dots are the experimental data, and the solid lines are the theoretical curves predicted by the two-state slow-kinetics model and the parameters in Table I. The curves have been displaced in the y axis for display purposes.

equilibrium population:

$$P'_u(T_0) = P_u(T_0) \quad (4)$$

For a two-state transition, at any temperature T_i the equilibrium population of molecules in the unfolded state is given by the equation:

$$P_u(T_i) = \exp[-\Delta G(T_i)/RT_i]/\{1 + \exp[-\Delta G(T_i)/RT_i]\} \quad (5)$$

where $\Delta G(T_i)$ is the Gibbs free energy of stabilization at the temperature T_i. The free energy of stabilization is a function of temperature as well as the activity of GuHCl as follows (Xie et al., 1991):

$$\Delta G(T_i) = \Delta G°(T_i) - RT_i\Delta n \ln(1 + K_b a_{GuHCl}) \quad (6)$$

where $\Delta G°(T_i) = \Delta H°(T_i) - T_i\Delta S°(T_i)$ is the free energy of stabilization in the absence of denaturant, K_b the association constant for GuHCl, a_{GuHCl} the activity of GuHCl, and Δn the difference in the number of GuHCl binding sites between the unfolded and native states of the protein. The activity of GuHCl was calculated using the mean ion activity coefficients published by Pace (1986) as described by Xie et al. (1991). The validity of the denaturant binding model has recently been tested by Makhatadze and Privalov (1992).

Equations 3–6 allow calculation of the observed population of molecules in the unfolded state at any temperature. The apparent excess enthalpy is obtained from the relationship $\langle\Delta H'\rangle = P'_u\Delta H$, and the observed excess heat capacity function from the temperature derivative of $\langle\Delta H'\rangle$. For the purpose of fitting the experimental data, the temperature dependence of the rate constant was phenomenologically represented by a polynomial expression of the form:

$$\ln k = a + b(T - 298.15) + c(T - 298.15)^2 \quad (7)$$

This form was found to be well-behaved numerically during the fitting procedures. Multidimensional analysis was performed for the data obtained at pH 5.3 since at this pH the transitions were highly reversible even at high GuHCl concentrations. The curves obtained at GuHCl concentrations smaller than 1 M in which the kinetic effects are not very pronounced were fitted globally. Up to 3 M GuHCl, each concentration set containing the data obtained at various scanning rates were fitted separately. The results of the nonlinear least-squares analysis of the data are shown in Figure 6, and the best-fitted parameters are summarized in Table I. It is clear from the data in Figure 6 that the simple two-state slow-kinetics model accurately accounts for the stability of

Table I: Results of Nonlinear Least-Squares Analysis of RNase T_1 Data as a Function of [GuHCl] and Scanning Rate

	[GuHCl] (M)				
	0/0.5/1.0	1.8	2.4	3	mean
$\Delta H°$(25 °C) (cal mol^{-1})	59600	59600	59600	59800	59600 ± 125[c]
$\Delta S°$(25 °C) (cal K^{-1} mol^{-1})	172.3	172.4	172.4	172.0	172.3 ± 0.2
ΔC_p (cal K^{-1} mol^{-1})	1181	1005	1261	1197	1160 ± 100
ΔH_b (cal mol^{-1})[a]	−2600	−2600	−2600	−2600	
K_b(25 °C) (M^{-1})	0.80	0.87	0.80	0.80	0.82 ± 0.03
Δn	14.4	13.7	14.0	14.0	14 ± 0.3
a[b]		−3.1	−2.9	−3.2	−3.1 ± 0.1
b[b]		−0.16	−0.16	−0.13	−0.15 ± 0.1
c[b]		0.01	0.01	0.01	0.01

[a] The enthalpy of GuHCl binding was not fitted. The value experimentally determined by Makhatadze and Privalov (1992) was used. [b] The phenomenological parameters a, b, and c for the polynomial expansion of the rate constants were not determined for the experiments at low GuHCl concentration in which the kinetic effects are small. [c] The quoted errors are the estimated uncertainties corresponding to 1 standard deviation of the mean values of the fitted parameters.

the protein as a function of temperature, GuHCl concentration, and scanning rate. Increasing the number of states of 3 did not significantly improve the goodness of the fit, indicating that the deviations between the observed and predicted data most likely arise from data reduction or instrumental errors rather than from the presence of other significantly populated states. More complex kinetic schemes were not considered since the limited time resolution of the calorimetric data does not support the resulting increase in the number of fitting parameters.

As seen in Table I, the intrinsic enthalpy as well as the intrinsic entropy values for unfolding are similar under all conditions studied and coincide within error with the values determined at zero GuHCl concentration. The parameters for zero GuHCl concentration are also in excellent agreement with values obtained previously by Shirley et al. (1989), Kielhaber et al. (1990d), and Hu et al. (1992). At 25 °C, the estimated association constant of GuHCl to the protein is 0.82 ± 0.03 M^{-1}. This value is also very close to values estimated earlier by different investigators (Pace, 1986; Xie et al., 1991; Makhatadze & Privalov, 1992). Also, the value of 14 for the number of additional GuHCl binding sites in the unfolded state is within the range expected for a protein the size of ribonuclease T_1. The average ΔC_p value obtained from the multidimensional analysis is 1.16 ± 0.1 kcal K^{-1} mol^{-1}. This value is somewhat lower than the value of 1.6 kcal K^{-1} mol^{-1} obtained from inspection of the calorimetric traces at zero GuHCl. This is not surprising given the difficulties in determining ΔC_p. Previously, Hu et al. (1992) have obtained values of 1.2 kcal K^{-1} mol^{-1} from the calorimetric traces and 1.59 kcal K^{-1} mol^{-1} from the temperature dependence of ΔH; Kiefhaber et al. (1990d) have reported a value of 1.22 kcal K^{-1} mol^{-1} from the temperature dependence of ΔH. It appears that the overall average, considering the data from different authors, is about 1.4 ± 0.2 kcal K^{-1} mol^{-1}. The agreement between the values estimated by multidimensional analysis of the calorimetric data with those values that have been determined independently strengthens the confidence in the validity of this approach.

Figure 7 summarizes the behavior of the unfolding rate constant as a function of temperature for the range covered in these studies. It must be noted that the values obtained from the polynomial representation of ln k should be considered valid only for the temperature interval covered by the experiments and that extrapolations outside this range must

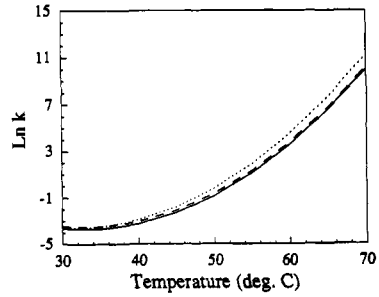

FIGURE 7: Temperature dependence of the natural logarithm of the rate constant for denaturation of Lys25-RNase T_1 at pH 5.3. The GuHCl molar concentrations are 1.8 (solid line), 2.4 (dashed line), and 3.0 (dotted line). The curves were calculated with the parameters in Table I as described in the text.

be taken with caution. This is especially true in this case because ribonuclease T_1, as well as other proteins, has a significant transition ΔC_p and exhibits a temperature of maximal stability and the phenomenon of cold denaturation. According to the thermodynamic parameters in Table I, in the absence of GuHCl, the temperature of maximal stability of ribonuclease T_1 is 5 °C, implying that the protein is destabilized both above and below that temperature. The rate constants plotted in Figure 7 depend both on temperature and on GuHCl concentration; however, the dependence appears to be stronger on temperature than on GuHCl concentration within the range studied ([GuHCl] < 3 M). These data suggest that the time constant for unfolding is intrinsically slow at low temperatures and that GuHCl further accentuates this behavior. Using a standard Arrhenius representation of the rate constant, we obtain an apparent enthalpy of activation on the order of 110 kcal mol^{-1} at 60 °C and an apparent activation heat capacity of about 4 kcal K^{-1} mol^{-1}. For the experiments at 3 M GuHCl in which the T_m extrapolated to zero scanning rate is 40.5 °C, the time constant for the unfolding reaction is on the order of 10 min. The effect of these slow kinetics can be appreciated in Figure 6, in which the transition curves obtained at 20 and 90 °C h^{-1} for 3 M GuHCl are separated by more than 5 °C. Perhaps the most dramatic example of the kinetic effect is given by the CD unfolding data in Figure 4. The CD unfolding curves were obtained under equilibrium conditions rather than "scanning" conditions. As seen in the figure, at 25 °C and pH 5.3, the midpoint of the transition occurs at 3.7 M GuHCl. This result should be compared with the calorimetric scans in Figures 2 and 6 clearly showing that at 25 °C there is still no evidence of a heat absorption process. However, simulation of the expected equilibrium heat capacity curve using the parameters in Table I indicates that at 25 °C the midpoint of the transition should occur at 3.3 M GuHCl, in excellent agreement with the experimental data. Previously, Kiefhaber et al. (1990a) have observed that the GuHCl-induced unfolding of ribonuclease T_1 at 10 °C and at pH 5.0 is characterized by a time constant of 3.9 h. These results are in agreement with our results and point to the fact that for ribonuclease T_1 not only the refolding kinetics but also the unfolding kinetics are very slow.

Structural Thermodynamic Calculations. Recently, a structural thermodynamic formalism aimed at predicting the stability of proteins from its crystallographic structure has been developed (Freire & Murphy, 1991; Murphy & Gill, 1991; Murphy & Freire, 1992; Freire et al., 1992; Murphy et al., 1992). This formalism has been shown to accurately account for the stability of the set of proteins for which structural and thermodynamic information is available (Murphy et al., 1992). According to this formalism, the quantity that has the most immediate correlation with the structure of the protein is the heat capacity change upon unfolding (ΔC_p), which is directly proportional to the degree of exposure to the solvent water of previously buried apolar and polar surfaces:

$$\Delta C_p = \Delta C_{p,ap} + \Delta C_{p,pol}$$

$$= (0.45 \pm 0.02)\Delta A_{ap} - (0.26 \pm 0.03)\Delta A_{pol} \quad (8)$$

where $\Delta C_{p,ap}$ and $\Delta C_{p,pol}$ are the apolar and polar contributions to the heat capacity change, respectively, ΔA_{ap} and ΔA_{pol} are the changes in the solvent-accessible apolar and polar surface areas, respectively, upon unfolding, and 0.45 and −0.26 are the elementary apolar and polar contributions, respectively, per mole of $Å^2$ in units of calories per degrees kelvin (Murphy & Freire, 1992; Murphy et al., 1992). Surface area calculations for ribonuclease T_1 were performed using the PDB file 1RNT as described in a previous paper (Murphy et al., 1992). According to these calculations, upon unfolding ribonuclease T_1 exposes to the solvent 5039 $Å^2$ of apolar surface and 3629 $Å^2$ of polar surface. These values predict a ΔC_p value of 1.33 ± 0.2 kcal K^{-1} mol^{-1}. Similar results are obtained by using the new atomic coordinates at 1.5-Å resolution (Martinez-Oyanedel et al., 1991). In this case, we obtain 5000 $Å^2$ of apolar surface and 3797 $Å^2$ of polar surface exposed to the solvent upon unfolding. These values predict a ΔC_p of 1.26 ± 0.2 kcal K^{-1} mol^{-1}. The experimental value obtained from the calorimetric traces at pH 5.3 and 7.0 in the absence of GuHCl is 1.6 ± 0.2 kcal K^{-1} mol^{-1}. The value obtained from the multidimensional analysis is 1.16 ± 0.1 kcal K^{-1} mol^{-1}. Previously determined values are 1.2 kcal K^{-1} mol^{-1} (Kiefhaber et al., 1990d), 1.2 ± 0.29 kcal K^{-1} mol^{-1} (determined from the C_p traces), and 1.59 kcal K^{-1} mol^{-1} (determined from the temperature dependence of ΔH) (Hu et al., 1992).

The polar and apolar contributions to the enthalpy and entropy changes upon unfolding are calculated in reference to the temperatures at which the apolar contributions to those terms are assumed to be zero, T_H^* and T_S^*. These temperatures have been estimated as 100 and 112 °C, respectively (Murphy & Gill, 1991; Murphy et al., 1992). Thus, the enthalpy change is

$$\Delta H = \Delta H^* + \Delta C_p(T - T_H^*) \quad (9)$$

where ΔH^* is the polar contribution to ΔH at T_H^*. The value for ΔH^* is directly proportional to the buried polar area and is given by the equation:

$$\Delta H^* = (35 \pm 3)\Delta A_{pol} \quad (10)$$

It has been shown that, for the protein thermodynamic database, eq 9 and 10 predict ΔH at the reference temperature of 60 °C with a standard deviation of ±6.6% (Murphy et al., 1992). Using the same equations for ribonuclease T_1, and the new atomic coordinates (Martinez-Oyanedel et al., 1991), we calculate a ΔH of 74 ± 7 kcal mol^{-1} at 53 °C, the transition temperature at pH 7.0. This value does not include any additional ionization or other effects. The experimental value at pH 7.0 in MOPS buffer is 84.5 kcal mol^{-1}, which is statistically higher, suggesting that other additional interactions contribute significantly to ΔH. The main candidates include protonation and ionization effects of the protein as well as the buffer. Of particular importance are the three anomalous histidines (His-92, His-40, and His-27 with pK_a's of 7.9, 7.8, and 7.2, respectively). If it is assumed that the enthalpy of ionization of these histidines is similar to that of standard histidines (7 kcal mol^{-1}) and taking the protonation

enthalpy of MOPS as −5 kcal mol^{-1}, an additional contribution on the order of 5 kcal mol^{-1} is expected for the transition at pH 7.0. This will bring the calculated value to 79 kcal mol^{-1}, which is closer to the experimental value of 84.5 kcal mol^{-1}. With the data at pH 5.3, the situation is similar. The experimental ΔH value at 60 °C is 91 kcal mol^{-1} in MES buffer while the calculated value at 60 °C is 82 ± 7 kcal mol^{-1}. This value includes the protonation of MES which is −3.71 kcal mol^{-1}. Therefore, assuming a zero enthalpy of ionization for the anomalous glutamic acids in ribonuclease T_1, the expected ΔH is on the order of 86 kcal mol^{-1}.

Finally, the experimental entropy change for ribonuclease T_1, extrapolated to the entropy convergence temperature of 112 °C, is 4.43 cal K^{-1} (mol of residues)$^{-1}$, which falls within the range of values obtained for the entire protein database [the average for the database is 4.3 ± 0.1 cal K^{-1} (mol of residues)$^{-1}$ at that temperature] (Murphy & Freire, 1992; Murphy et al., 1992).

CONCLUSIONS

These studies have shown that from a thermodynamic point of view, ribonuclease T_1 behaves in a manner that resembles other globular proteins. Only the enthalpy change appears to be about 10 kcal mol^{-1} larger than the expected value for a globular protein of similar molecular weight and structure. However, this effect can be rationalized in terms of the known ionization behavior of ribonuclease T_1. Currently, we are performing calorimetric measurements using buffers with different heats of ionization in order to experimentally dissect the enthalpic contributions to the folding/unfolding equilibrium. The most surprising feature of the thermal unfolding transition has been its kinetic behavior at low temperatures. To the best of our knowledge, we know of no other globular protein that exhibits a reversible unfolding transition as slow as the one observed here for ribonuclease T_1.

REFERENCES

Arni, R., Heinemann, U., Maslowska, M., Tokuoka, R., & Saenger, W. (1987) *Acta Crystallogr., Sect. B B43*, 548–554.

Arni, R., Heinemann, U., Tokuoka, R., & Saenger, W. (1988) *J. Biol. Chem. 263*, 15358–15368.

Eigen, M., & de Maeyer, L. (1963) in *Techniques of Organic Chemistry*, Vol. III, Part II, pp 895–1054, John Wiley & Sons, New York.

Flogel, M., & Biltonen, R. L. (1975) *Biochemistry 14*, 2603–2609.

Freire, E. (1989) *Comments Mol. Cell. Biophys. 6*, 123–140.

Freire, E., & Biltonen, R. L. (1978) *Biopolymers 17*, 463–479.

Freire, E., & Murphy, K. P. (1991) *J. Mol. Biol. 222*, 687–698.

Freire, E., Murphy, K. P., Sanchez-Ruiz, J. M., Galisteo, M. L., & Privalov, P. L. (1992) *Biochemistry 31*, 250–256.

Heinemann, U., & Saenger, W. (1982) *Nature 299*, 27–31.

Heinemann, U., Wernitz, M., Pahler, A., Saenger, W., Menke, G., & Ruterjans, H. (1980) *Eur. J. Biochem. 109*, 109–114.

Hu, C. Q., Sturtevant, J. M., Thomson, J. A., Erickson, R. E., & Pace, C. N. (1992) *Biochemistry 31*, 4876–4882.

Inagaki, F., Kawano, Y., Shimada, I., Takahashi, K., & Miyazawa, T. (1981) *J. Biochem. (Tokyo) 89*, 1185.

Kiefhaber, T., & Schmid, F. X. (1992) *J. Mol. Biol. 224*, 231–240.

Kiefhaber, T., Quaas, R., Hahn, U., & Schmid, F. X. (1990a) *Biochemistry 29*, 3053–3061.

Kiefhaber, T., Quaas, R., Hahn, U., & Schmid, F. X. (1990b) *Biochemistry 29*, 3061–3070.

Kiefhaber, T., Grunert, H., Hahn, U., & Schmid, F. X. (1990c) *Biochemistry 29*, 6475–6480.

Kiefhaber, T., Schmid, F. X., Renner, M., Hinz, H.-J., Hahn, U., & Quaas, R. (1990d) *Biochemistry 29*, 8250–8257.

Koepke, J., Maslowska, M., Heinemann, U., & Saenger, W. (1989) *J. Mol. Biol. 206*, 475–488.

Kostreva, D., Choe, H. W., Heinemann, U., & Saenger (1989) *Biochemistry 28*, 7592–7600.

Kuwajima, K. (1989) *Proteins: Struct., Funct., Genet. 6*, 87–103.

Lentz, B., Freire, E., & Biltonen, R. L. (1978) *Biochemistry 17*, 4475–4480.

Makhatadze, G., & Privalov, P. L. (1990) *J. Mol. Biol. 213*, 375–384.

Makhatadze, G., & Privalov, P. L. (1992) *J. Mol. Biol. 226*, 491–505.

Martinez-Oyanedel, J., Choe, H. W., Heinemann, U., & Saenger, W. (1991) *J. Mol. Biol. 222*, 335–352.

McNutt, M., Mullins, L. S., Raushel, F. M., & Pace, C. N. (1990) *Biochemistry 29*, 7572–7576.

Murphy, K. P., & Gill, S. J. (1991) *J. Mol. Biol. 222*, 699–709.

Murphy, K. P., & Freire, E. (1992) *Adv. Protein Chem.* (in press).

Murphy, K. P., Xie, D., Bhakuni, V., & Freire, E. (1992) *J. Mol. Biol. 227*, 293–306.

Oobatake, M., Takahashi, S., & Ooi, T. (1979) *J. Biochem. 86*, 65–70.

Pace, C. N. (1986) *Methods Enzymol. 131*, 266–280.

Pace, C. N., & Grimsley, G. R. (1988) *Biochemistry 27*, 3242–3246.

Pace, C. N., Grimsley, G. R., & Barnett, B. J. (1987) *Anal. Biochem. 167*, 418–422.

Pace, C. N., Grimsley, G. R., Thomson, J. A., & Barnett, B. J. (1988) *J. Biol. Chem. 263*, 11820–11825.

Pace, C. N., Laurents, D. V., & Thomson, J. A. (1990) *Biochemistry 29*, 2564–2572.

Ramsay, G., & Freire, E. (1990) *Biochemistry 29*, 8677–8683.

Sanchez-Ruiz, J. M., Lopez-Lacomba, J. L., Cortijo, M., & Mateo, P. L. (1988) *Biochemistry 27*, 1648–1652.

Sander, C., & Ts's, P. O. P. (1971) *Biochemistry 10*, 1953–1966.

Shirley, B. A., & Laurents, D. V. (1990) *J. Biochem. Biophys. Methods 20*, 181–188.

Shirley, B. A., Stanssens, P., Steyaert, J., & Pace, C. N. (1989) *J. Biol. Chem. 264*, 11621–11625.

Straume, M., & Freire, E. (1992) *Anal. Biochem. 203*, 259–268.

Sugio, S., Amisaki, T., Ohishi, H., & Tomita, K. (1988) *J. Biochem. (Tokyo) 103*, 354–366.

Xie, D., Bhakuni, V., & Freire, E. (1991) *Biochemistry 30*, 10673–10678.

Registry No. Rnase T_1, 9026-12-4; GuHCl, 50-01-1.